

Enhanced Quasiparticle Relaxation in a Superconductor via the Proximity Effect

Kevin M. Ryan and Venkat Chandrasekhar*

Northwestern University Department of Physics & Astronomy, Evanston Illinois, 60208, USA

(Dated: September 10, 2024)

Quasiparticle relaxation in pure superconductors is thought to be determined by the intrinsic inelastic scattering rate in the material. In certain applications, *i.e.* superconducting qubits and circuits, excess quasiparticles exist at densities far beyond the thermal equilibrium level, potentially leading to dephasing and energy loss. In order to engineer superconductors with shorter overall quasiparticle lifetimes, we consider the impact of a proximity layer on the transport of quasiparticles in a superconductor. We find that a normal metal layer can be used to significantly increase the relaxation rate of quasiparticles in a superconductor, as seen by a large reduction in the quasiparticle charge imbalance in a fully proximitized Cu/Al bilayer wire. The mechanism for this effect may be useful for preventing quasiparticle poisoning of qubits using carefully chosen proximity bilayers consisting of clean superconductors and disordered normal metals.

Quasiparticle excitations are a persistent issue in the development of several superconducting technologies [1–4], including superconducting qubits. Contributing to energy dissipation and dephasing, excess quasiparticles limit the lifetime of qubits and degrade their performance [5–7]. Despite predictions that their density should be exponentially suppressed at the operating temperature of current superconducting quantum computers, many reports indicate populations of quasiparticles orders of magnitude higher than expected [5, 6, 8–11]. This vast discrepancy has lead to many proposals for the origin of these excess quasiparticles, ranging from infrared-light leaks and resonant coupling to microwave signals [12–14]; stress induced phonon bursts [15] or cosmic radiation [16]; pair-breaking due to magnetic defects [17, 18] or by non-magnetic defects in the presence of intrinsic gap-anisotropy [19–21]. Often, these proposed mechanisms rely sensitively on materials properties of the superconductor that are difficult (if not impossible) to engineer, or on extrinsic sources which cannot be mitigated via improved circuit design or avoided via quantum error correction [22]. As the origin of this “quasiparticle poisoning” continues to be debated, it seems unlikely that any one solution will prevent the generation of quasiparticles, and instead, new focus is being placed on engineering their dynamic behavior and relaxation.

Fortunately, the study of how quasiparticles diffuse and relax within superconductors is an old one, dating back to original works by Clark and Tinkham [23–26] and others [27, 28] exploring the relaxation rate of quasiparticles in superconductors among other non-equilibrium effects [29]. In many of these studies, the superconductors are deliberately driven out of equilibrium by an injected current from a normal metal to either enhance [30] or suppress [31] their superconductivity. As a net charge is in-

jected, this also leads to an imbalance between electron- and hole-like quasiparticle populations that shifts the chemical potential for quasiparticles vs. Cooper-pairs [29, 32–34], permitting simultaneous control over several degrees of freedom of their non-equilibrium distribution. Only relatively recently have these types of experiments been performed at mK temperatures[34–37], but these well established techniques for generation and detection of quasiparticles have seldom been implemented to study quasiparticle poisoning in superconducting qubits.

Instead, much work currently focuses on a variety of quasiparticle trapping schemes intended to divert quasiparticles within qubits. Such experiments typically focus on extracting quasiparticles into discrete normal metal reservoirs which are only weakly attached to qubits [38–40], with their efficacy determined via qubit operation. Several recent works attempting to mitigate other issues in superconducting qubits, such as surface-oxide induced dielectric loss, have also begun to successfully employ normal metal encapsulation of the entire surface of the device [41, 42]. In both cases, little information can be extracted about the quasiparticles themselves. This is especially relevant for encapsulated qubits, where the proximity effect present along this extended, highly transparent interface raises questions about how quasiparticles may behave dynamically in the presence of a spatially non-uniform superconducting gap. While it has already been proposed that the gap suppression induced by the inverse proximity effect can have either a positive or negative effect on transmon qubit performance [43–45] depending on the sample geometry, relatively little work has directly examined the relaxation of non-equilibrium quasiparticles directly within such a bilayer. To explore this issue, we present in this Letter a comparative study of charge imbalance in a simple Al device and one consisting of an Al/Cu (20nm/3nm) proximity effect bilayer. Using tunneling methods derived from the foundational studies in non-equilibrium superconductivity, our results

* v-chandrasekhar@northwestern.edu

demonstrate a clear and substantial increase in the relaxation rate of quasiparticles in the presence of the inverse proximity effect.

Charge and energy imbalance, being the first observed signatures of non-equilibrium superconductivity, can provide direct access to inelastic scattering rates/lifetimes for quasiparticles in a given system. In most studies, charge imbalance is generated via injection of charged quasiparticle distributions through Normal-Insulator-Superconductor ('NIS') tunnel junctions. In Clark's original experiment [23], NIS and SIS junctions were co-located on the same superconducting wire, and used to drive and measure a steady-state, non-equilibrium quasiparticle distribution $f_k(\epsilon_k)$ [32, 33]. In this case, when injecting a current of predominantly electron or hole-like Bogoliubov quasiparticles across the NIS junction, one can calculate the accrued charge imbalance Q^* by integrating the total charge of all quasiparticles

$$Q^* \equiv \int_{-\infty}^{\infty} q_k f_k(\epsilon_k) d\epsilon_k. \quad (1)$$

This total charge is compensated by a change in the chemical potential of the superconductor [32, 33]

$$\mu_{Q^*} = \frac{Q^*}{2eN(0)}, \quad (2)$$

which can be independently detected and compared to the chemical potential for Cooper pairs. This is often done by observing the current across a second NIS junction, $I = G^N \times \mu_{Q^*}$, which by Eq. 1 will contain contributions from all energies, being non-zero only in the presence of charge imbalance.

In 2010 Hübner *et al.* [35] demonstrated a succinct experimental model to directly measure the real space relaxation of quasiparticle charge imbalance at mK temperatures relevant for superconducting quantum applications, which serves as a fundamental basis for both the experimental design and analysis to follow. By using pairs of NIS tunnel junctions biased to specific voltages, they demonstrated that a non-local current due to charge imbalance alone could be detected away from the injector junction with sufficient amplitude to determine the spectral properties of the charge imbalance relaxation length in Al at low temperatures. To summarize the process: first, a current $I_{inj}(V_{inj})$ is injected at a given bias to generate a charge imbalance Q^* by tunneling of electrons or holes into the superconductor which then relax at a rate of $1/\tau_{Q^*}$. For large injector currents, a large charge imbalance Q^* will be established and $d\mu_{Q^*}/dV_{inj}$ will be nonzero. Due to the diffusion of quasiparticles through the superconductor, μ_{Q^*} will decay exponentially over a length scale $\lambda_{Q^*} = \sqrt{D\tau_{Q^*}}$ where D_q is the diffusion constant for quasiparticles. Finally, one observes the steady-state quasiparticle current $dI_{det}/dV_{inj} = G_{det}^N \times d\mu_{Q^*}/dV_{inj}$ using a second, unbiased NIS junction a distance L from the injector. By

measuring at zero detector bias, this current stems entirely from the chemical potential within the superconductor due to charge imbalance alone, and by making multiple measurements at varying L , the exponential relaxation can be traced out. More detailed derivations of the quasiparticle conductance between junctions have been presented extensively elsewhere in the literature [29, 32, 33, 35, 46].

In order to compare the quasiparticle conductance both with and without the influence of the inverse proximity effect, a pair devices consisting of 6 junctions spaced between 2 and 6 μm apart with a maximum separation of 20 μm were fabricated using a conventional PMGI/PMMA bilayer e-beam lithography process on 1 μm SiO_2 substrates. A false color SEM micrograph of the Al/Cu bilayer device is shown as part of Fig. 1. All lithography was performed in a single step, whereby the written pattern encompasses the central wire and junctions, leads, and wirebonding pads such that during metallization a continuous film is formed which prevents the introduction of parasitic tunnel junctions in the leads. Only the desired Al or Al/Cu bilayer wire spans the full width of the junction region. This is done by using a very minimal PMGI undercut so that metalization layers

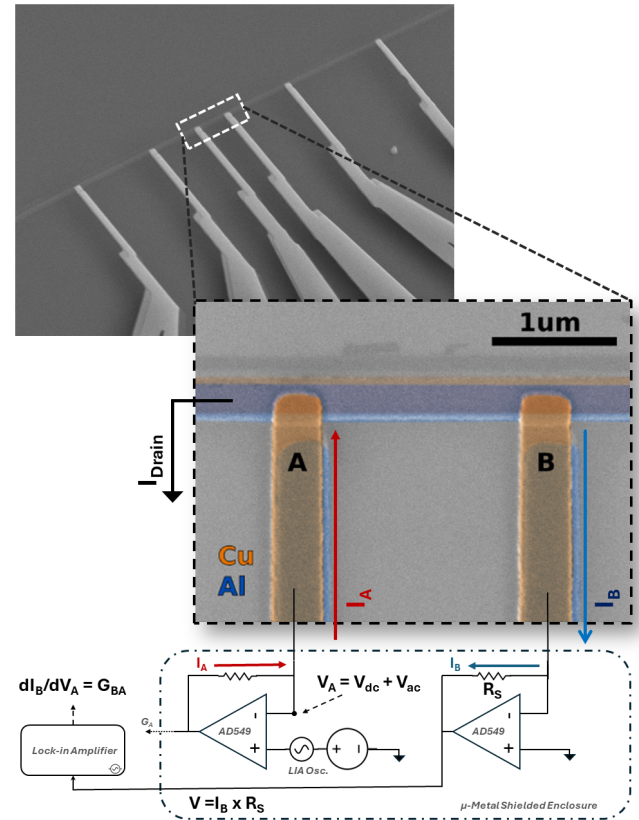


FIG. 1. Top: False-color SEM micrograph of the inner-most pair of leads on the bilayer device, and a circuit diagram of the voltage biased current pre-amplifiers used for conductance measurements.

are deposited on the resist sidewall and removed during liftoff.

All metalization was performed using a multi-pocket e-beam evaporator with a base pressure of 3×10^{-7} Torr or lower at ambient temperatures, with film thicknesses monitored via crystal monitor during deposition. To form the control device, deposition was performed of the Al at a 0° incidence, followed immediately by dynamic oxidation in 130 mTorr of flowing 99.994% O₂ gas for 15 minutes. Subsequently, 80 nm of Cu was deposited upwards over the Al at 35° , followed by 3 nm of Ti which helps prevent oxidation of the Cu during liftoff and storage. To form the bilayer device, an identical procedure is followed except that 3 nm of Cu was deposited at an upwards angle of 10° before the Al to prevent short circuiting to the normal metal leads. Great care was taken to match deposition pressures/rates and oxidation conditions between the two devices. Liftoff was performed with alternating baths of hot acetone and an NMP based remover, followed by ultrasonication in acetone and isopropanol to remove the metalized sidewall. The substrates were then cleaved to size, imaged via SEM, and wirebonded before being immediately cooled to 77 K. Although we have not noticed degradation of Al/Cu based devices made in this fashion, the control device was stored under vacuum during fabrication of the bilayer device, and both devices were fabricated within 48 hours of cooldown.

Measurements were performed using a ³He/⁴He dilution refrigerator with a base temperature of approximately 19 mK. Each measurement line has 20Ω of series lead resistance at base temperature, and is filtered with an 800 kHz π -filter. All pre-amplifiers are battery powered and housed in a μ -metal enclosure immediately beside the dilution refrigerator, which is connected via a μ -metal shielded cable. Both grounding and vibration isolation have been carefully considered and are essential to obtaining low electronic temperatures given the large number of connections for each device. Differential measurements were performed using standard lock-in techniques.

Both single and dual-junction conductance measurements were performed using custom voltage biased transimpedance amplifiers based on AD549 electrometer op-amps with an input impedance of $10^{13}\Omega$ and a gain of 10^7 V/A. A combined ac+dc bias was produced via a lock-in amplifier and function generator, with ac excitation of 1 to 5 μ V depending on the full scale sensitivity for a given measurement. A schematic of the dual-conductance measurement used is shown in Fig. 1. In short, independent dc-biases are applied to a pair of junctions A/B with ac-excitation at frequency f_A and f_B respectively. With the A-junction being closer to the ground point of the circuit than the B-junction, this should eliminate any conventional current from passing from A to B, however quasiparticle current and super

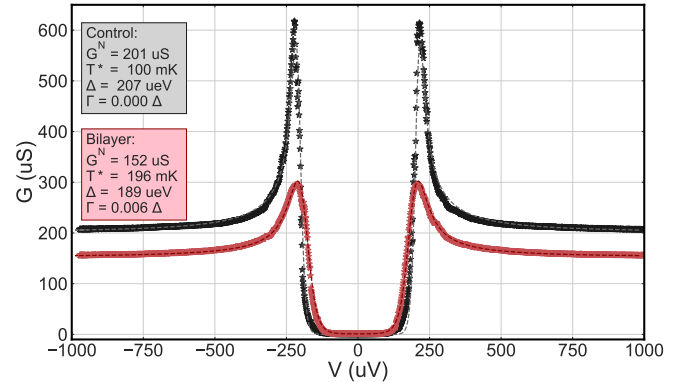


FIG. 2. Conductance measurements and Dynes-type fits for two junctions from both the control and bilayer devices, taken with identical measurement configurations at a bath temperature of 20 mK. Both the Dynes parameter Γ and T are unconstrained.

current can coexist in the region of junction B and allow for the conductance measurement $G_{BA} \equiv dI_B/dV_A$. Simultaneous measurements of the junction conductances G_A and G_B were also performed to characterize the local behavior of the junctions. Note that, due to input voltage offsets, small bias corrections of 10 to 20 μ V have been made to ensure the symmetry of G_A and G_B . The resistance across the Al or Al/Cu wire itself was obtained via a 4-terminal resistance measurement with an excitation of 100 nA.

We first qualify both the intrinsic quality of the junctions and the impact of the Cu layer on the superconducting density of states in the bilayer. Fig. 2 shows example fits for corresponding junctions on both the control and bilayer devices, measured in the lowest noise configuration where all other junctions are shorted to ground. This was found to somewhat reduce the electronic temperature, increasing the coherence peak's prominence. In all junctions, we find strong NIS-type features, with only a small spread in normal state conductance which we attribute to variations in the overlap areas.

In both devices, a fully developed gap is seen at the operating bath temperature of 20 mK, but the coherence maxima in the conductance are suppressed in the bilayer. Example fits are shown using a Dynes-type model of the superconducting density of states to calculate the conductance [47, 48]. This gives an effective electronic temperature of 100 mK for the control, consistent with incomplete thermalization of the electrons within the sample due to thermal radiation or noise. In the bilayer the apparent thermal broadening of the conductance maxima can be fit to ≈ 200 mK, which is most likely due to spatial inhomogeneity in the gap Δ across the junction caused by the intentional offset between the Cu and Al layers.

Along with suppression of the gap, the inverse proximity effect causes a corresponding decrease in T_c , shown in

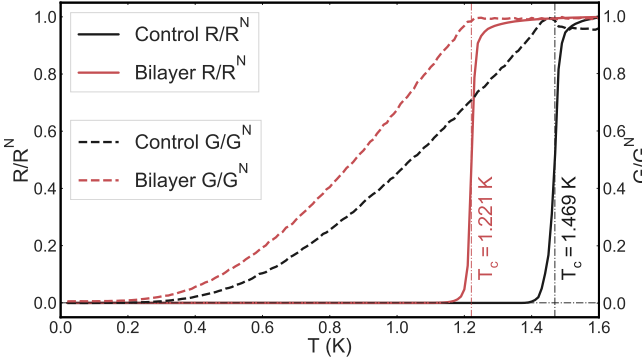


FIG. 3. Resistance of the superconducting/bilayer wire, and conductance of their corresponding junctions normalized to their maxima below 1.6K.

Fig. 3. The inclusion of the Cu layer causes a reduction in T_c from 1.47 K to 1.22 K (taking T_c to be the value where $R/R^N = 0.5$), a suppression of $\approx 17\%$. Assuming the bilayer to have an transparent NS interface, quasi-classically we would expect a suppression of only 13% for a 3 nm/20 nm NS bilayer. This suggests that the slight offset between the layers causes an enhancement of the inverse proximity effect, in agreement with the tunneling results suggesting spatial variation of the gap.

Next we consider the signatures of charge imbalance in dual junction experiments measuring G_{BA} for both devices. As both the injected and extracted quasiparticle currents scale in magnitude with the intrinsic conductance of the junction, we must account also for differences between chosen junctions in addition to their separation to fully describe the charge imbalance effect measured. To do so, we employ the model of Hübler *et al.* [35], which provides an approximate functional form for the conductance between junctions separated by a distance L :

$$G_{BA} = g^*(eV_A) G_B^N G_A^N \frac{\rho_N \lambda_{Q^*}}{2A} e^{-L/\lambda_{Q^*}}, \quad (3)$$

or equivalently:

$$\frac{2l}{R_N} \frac{G_{BA}}{G_A^N G_B^N} = g^*(eV_A) \lambda_{Q^*} e^{-L/\lambda_{Q^*}}, \quad (4)$$

where A (l) is the cross sectional area (length) of the central wire, ρ_N (R_N) is the normal state resistivity (resistance) of the wire and g^* is a dimensionless shape function on the order of unity associated with the BCS density of states and thermal broadening, being approximately zero for $eV_A < \Delta$ when no quasiparticle current is injected.

The normalization performed in Eq. 4 is convenient as it accounts for differences in the resistance of the wires, and eliminates the cross sectional area A which is harder to determine than the wire length of $l = 22 \mu\text{m}$ for both devices. These normalized data are shown in Fig. 4. As

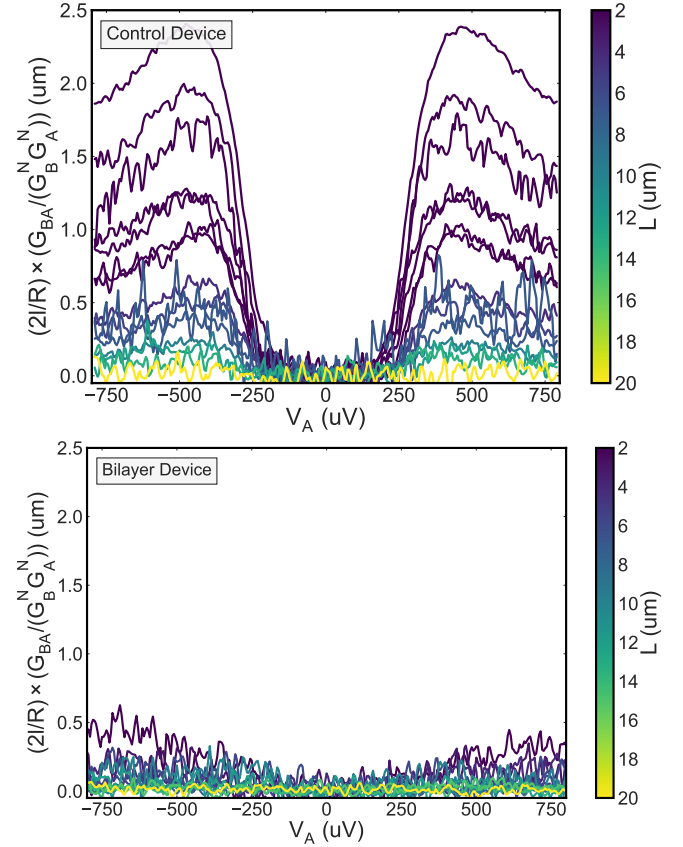


FIG. 4. Normalized quasiparticle conductance measurements of all pairs of junctions on the control device (top) and the bilayer device (bottom).

expected for charge imbalance, G_{BA} is generally symmetric with respect to V_A and appears only for $V_A > \Delta$. In the control device we can observe a quasiparticle conductance over $L \leq 15 \mu\text{m}$ that is clearly suppressed in the bilayer. We also note that the resistance of the proximity bilayer ($R^N = 586 \Omega$) is slightly larger in the normal state than that of the control ($R^N = 497 \Omega$), possibly due to the inclusion of additional defects at the time of deposition which could suppress T_c .

We can further isolate the energy and length dependence by performing cuts of the data at specific injector voltages, and plot them logarithmically as a function of L , as shown in Fig. 5. In this comparison, the exponential relaxation over an energy dependent length λ_{Q^*} is clearly seen in the Al control device, and is generally consistent with previous reports [35]. Again, we see a near complete suppression of the quasiparticle conductance lengthscale in the bilayer device, being suppressed by over an order of magnitude and within the experimental noise limit beyond $\approx 4 \mu\text{m}$.

For quasiparticle injection at energies sufficiently above the gap that a detectable charge imbalance is generated, we can fit the control results to Eq. 4 to obtain an estimate of λ_{Q^*} shown in Fig. 6. Due to the very weak ex-

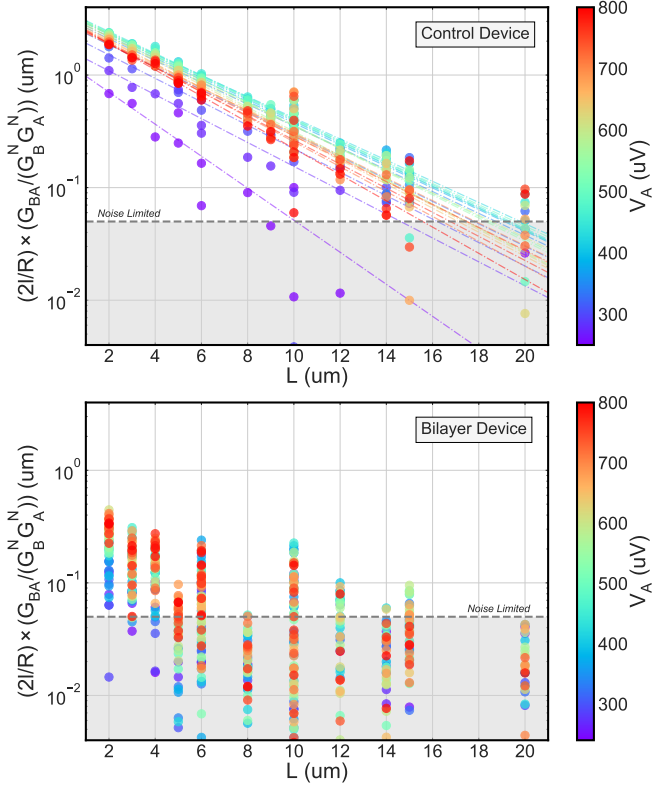


FIG. 5. Results from Fig. 4, interpolated to specific values V_A and re-plotted as a function of junction separation L on a logarithmic scale for both the control (top) and bilayer (bottom) devices. The dashed lines for the control device are fits to Eq. 4 for values $eV_A \gtrsim \Delta$. The grey region indicates an estimated minimum noise threshold of $\approx 0.05 \mu\text{m}$ which limits the range of the data.

ponential dependence in the bilayer sample, it is not possible to reliably extract λ_{Q^*} with the available data, but through comparison between the devices, Eq. 4 would suggest it may be $\approx 1 \mu\text{m}$ or less.

When taken together with the proximity effect evidenced by the suppression of T_c and Δ , the near total lack of quasiparticle conductivity clearly demonstrates that the introduction of a simple proximitized Cu layer to an Al superconducting wire can cause dramatic enhancement of the relaxation of quasiparticles and their charge imbalance. At the same time, the bilayer remains robustly superconducting at base temperature. We can understand this effect by considering the role of both layers in quasiparticle relaxation.

In an ordinary superconductor near T_c , the charge imbalance relaxation rate scales with the superconductor's intrinsic inelastic scattering rate for electrons τ_E^{-1} [33]

$$\tau_{Q^*} = \frac{4k_B T_c}{\pi \Delta(T)} \times \tau_E. \quad (5)$$

This diverges near T_c at the gap closes, which in turn yields a maxima in the charge imbalance length just be-

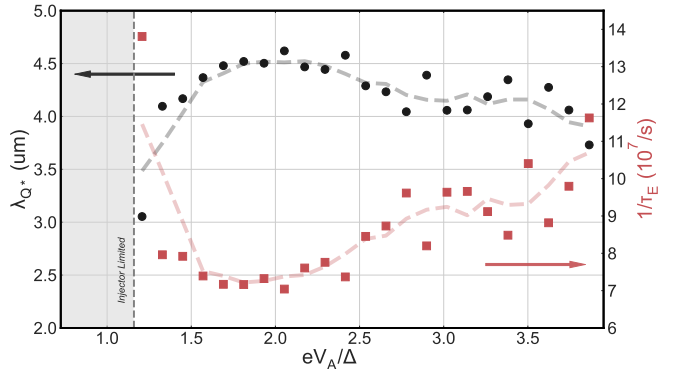


FIG. 6. $\lambda_{Q^*}(V_A)$ (black circles) obtained by fitting the control results shown in Fig. 5 to Eq. 4, and τ_E (red squares) from Eq. 5 (see Appendix). The grey region indicates energies where insufficient current I_A is injected to measure λ_{Q^*}

low the transition. For $T \ll T_c$, it has been argued that this expression still holds to within a good approximation due to simultaneous energy relaxation and conversion between electron and hole-like quasiparticles [24]. As $T \rightarrow 0$, $\Delta(T) \rightarrow \Delta_0 \approx 1.7k_B T_c$ and the rate saturates to a constant factor of τ_E . Therefore T_c suppression alone would not be expected to provide the substantial modification of the charge imbalance seen here.

For proximity bilayers, determining the inelastic scattering rate becomes theoretically complicated. A quasiclassical treatment of the problem by Golubov and Houweman [49] for a bilayer similar to one studied here also yields only a weak logarithmic modification of the quasiparticle relaxation rate in the superconductor due to proximity suppression of T_c . However, they additionally establish that the effective relaxation rate for quasiparticles in an inhomogenous system consisting of a superconductor S and a thinner bilayer of a superconductor S' (in our case, Al and proximitized Cu) will be modified if the intrinsic relaxation rates between the two are different, having quasiparticle relaxation rates τ_{0S}^{-1} and $\tau_{0S'}^{-1}$. This effective rate τ_{eff} was found to be determined by a parallel contributions from both layers as:

$$\frac{1}{\tau_{eff}} = \frac{1.82}{d_S} \left[\frac{L_{eff}}{\tau_{0S}} + \frac{L'_{eff}}{\tau_{0S'}} \right] \frac{A'}{A}, \quad (6)$$

where d_S is the thickness of the superconductor "S layer" and L_{eff}/L'_{eff} are effective thicknesses and A/A' the area of the S and S' layers respectively. They further argue that for a clean interface, the effective quasiparticle relaxation time is almost exclusively determined by the *smaller* of the two relaxation times.

Under this assumption, it should be possible to tune the T_c and τ_{eff}^{-1} of a superconductor independently using an NS bilayer so as to engineer faster quasiparticle relaxation while the entire device remains robustly superconducting. In our device, the Cu layer is thin enough that T_c suppression is relatively small, but also

has an intrinsically higher scattering rate (or is significantly disordered enough) to enhance the relaxation of quasiparticles across the entire superconductor (see Appendix for further details). As this yields an observable decrease in an injected charge imbalance, this may also be a promising avenue for reducing the density of the bulk non-equilibrium quasiparticles responsible for quasiparticle poisoning without substantially reducing T_c or generating large normal-metal regions across a qubit. This may be especially useful in the construction of Josephson junctions within qubits, as these are typically constructed from Al and could readily be adjusted to include a normal metal layer in their design. We suggest further studies via both dc-transport and RF-quasiparticle detection in disordered metal/superconductor bilayers to determine the exact benefits of such an approach.

In conclusion, we have observed a significant modification of the quasiparticle conductance within a superconducting Al wire via addition of a fully proximitized Cu underlayer. In both samples we find that the superconducting density of states seen via tunneling can be explained via a simple Dynes-type fit, albeit with a gap that appears excessively broadened due to an inhomogeneous gap. Using a dual-junction conductance measurement we report the absence of significant charge imbalance compared to the control device. This effect is not explained by pure T_c suppression due to the inverse proximity effect, but by quasiclassical predictions indicating a strong tunability of the quasiparticle relaxation rate in a proximity effect bilayer. Given these findings, we predict that, for a sufficiently diffusive normal metal, the proximity effect could be used to artificially enhance the relaxation rate of quasiparticles in a superconductor without significantly reducing Δ . Such enhancement may permit engineering of superconductors with lower quasiparticle populations at mK temperatures to help address quasiparticle poisoning in superconducting qubits.

Acknowledgments— This material is based upon work supported by the U.S. Department of Energy, Office of Science, National Quantum Information Science Research Centers, Superconducting Quantum Materials and Systems Center (SQMS) under contract no. DE-AC02-07CH11359.

Poisoning of Majorana Qubits, Physical Review Letters **126**, 057702 (2021).

- [4] A. E. Svetogorov, D. Loss, and J. Klinovaja, Quasiparticle poisoning in trivial and topological Josephson junctions, Physical Review B **105**, 174519 (2022).
- [5] K. Serniak, *Nonequilibrium Quasiparticles in Superconducting Qubits*, Ph.D. thesis, Ph. D. thesis, Yale University (2019).
- [6] L. Glazman and G. Catelani, Bogoliubov quasiparticles in superconducting qubits, SciPost Physics Lecture Notes , 31 (2021).
- [7] J. Aumentado, G. Catelani, and K. Serniak, Quasiparticle poisoning in superconducting quantum computers, Physics Today **76**, 34 (2023).
- [8] J. Aumentado, M. W. Keller, J. M. Martinis, and M. H. Devoret, Nonequilibrium Quasiparticles and \$2e\\$ Periodicity in Single-Cooper-Pair Transistors, Physical Review Letters **92**, 066802 (2004).
- [9] J. M. Martinis, M. Ansmann, and J. Aumentado, Energy Decay in Superconducting Josephson-Junction Qubits from Nonequilibrium Quasiparticle Excitations, Physical Review Letters **103**, 097002 (2009).
- [10] G. Catelani, J. Koch, L. Frunzio, R. J. Schoelkopf, M. H. Devoret, and L. I. Glazman, Quasiparticle Relaxation of Superconducting Qubits in the Presence of Flux, Physical Review Letters **106**, 077002 (2011).
- [11] P. J. de Visser, J. J. A. Baselmans, P. Diener, S. J. C. Yates, A. Endo, and T. M. Klapwijk, Number Fluctuations of Sparse Quasiparticles in a Superconductor, Physical Review Letters **106**, 167004 (2011).
- [12] A. D. Córcoles, J. M. Chow, J. M. Gambetta, C. Rigetti, J. R. Rozen, G. A. Keefe, M. Beth Rothwell, M. B. Ketchen, and M. Steffen, Protecting superconducting qubits from radiation, Applied Physics Letters **99**, 181906 (2011).
- [13] R. Barends, J. Wenner, M. Lenander, Y. Chen, R. C. Bialczak, J. Kelly, E. Lucero, P. O’Malley, M. Mariantoni, D. Sank, H. Wang, T. C. White, Y. Yin, J. Zhao, A. N. Cleland, J. M. Martinis, and J. J. A. Baselmans, Minimizing quasiparticle generation from stray infrared light in superconducting quantum circuits, Applied Physics Letters **99**, 113507 (2011).
- [14] C. H. Liu, D. C. Harrison, S. Patel, C. D. Wilen, O. Raferty, A. Shearow, A. Ballard, V. Iaia, J. Ku, B. L. T. Plourde, and R. McDermott, Quasiparticle Poisoning of Superconducting Qubits from Resonant Absorption of Pair-Breaking Photons, Physical Review Letters **132**, 017001 (2024).
- [15] R. Anthony-Petersen, A. Biekert, R. Bunker, C. L. Chang, Y.-Y. Chang, L. Chaplinsky, E. Fascone, C. W. Fink, M. Garcia-Sciveres, R. Germond, W. Guo, S. A. Hertel, Z. Hong, N. Kurinsky, X. Li, J. Lin, M. Lisovenko, R. Mahapatra, A. Mayer, D. N. McKinsey, S. Mehrotra, N. Mirabolfathi, B. Neblosky, W. A. Page, P. K. Patel, B. Penning, H. D. Pinckney, M. Platt, M. Pyle, M. Reed, R. K. Romani, H. Santana Queiroz, B. Sadoulet, B. Serrfass, R. Smith, P. Sorensen, B. Suerfu, A. Suzuki, R. Underwood, V. Velan, G. Wang, Y. Wang, S. L. Watkins, M. R. Williams, V. Yefremenko, and J. Zhang, A stress-induced source of phonon bursts and quasiparticle poisoning, Nature Communications **15**, 6444 (2024).
- [16] A. P. Vepsäläinen, A. H. Karamlou, J. L. Orrell, A. S. Dogra, B. Loer, F. Vasconcelos, D. K. Kim, A. J. Melville, B. M. Niedzielski, J. L. Yoder, S. Gustavsson, J. A. For-

- [1] U. Patel, I. V. Pechenezhskiy, B. L. T. Plourde, M. G. Vavilov, and R. McDermott, Phonon-mediated quasiparticle poisoning of superconducting microwave resonators, Physical Review B **96**, 220501 (2017).
- [2] S. M. Albrecht, E. B. Hansen, A. P. Higginbotham, F. Kuemmeth, T. S. Jespersen, J. Nygård, P. Krogstrup, J. Danon, K. Flensberg, and C. M. Marcus, Transport Signatures of Quasiparticle Poisoning in a Majorana Island, Physical Review Letters **118**, 137701 (2017).
- [3] T. Karzig, W. S. Cole, and D. I. Pikulin, Quasiparticle

maggio, B. A. VanDevender, and W. D. Oliver, Impact of ionizing radiation on superconducting qubit coherence, *Nature* **584**, 551 (2020).

[17] P. Kumar, S. Sendelbach, M. A. Beck, J. W. Freeland, Z. Wang, H. Wang, C. C. Yu, R. Q. Wu, D. P. Pappas, and R. McDermott, Origin and Reduction of $1/f$ Magnetic Flux Noise in Superconducting Devices, *Physical Review Applied* **6**, 041001 (2016).

[18] M. V. P. Altoé, A. Banerjee, C. Berk, A. Hajar, A. Schwartzberg, C. Song, M. Alghadeer, S. Aloni, M. J. Elowson, J. M. Kreikebaum, E. K. Wong, S. M. Griffin, S. Rao, A. Weber-Bargioni, A. M. Minor, D. I. Santiago, S. Cabrini, I. Siddiqi, and D. F. Ogletree, Localization and Mitigation of Loss in Niobium Superconducting Circuits, *PRX Quantum* **3**, 020312 (2022).

[19] P. J. Hirschfeld, P. Wölfe, J. A. Sauls, D. Einzel, and W. O. Putikka, Electromagnetic absorption in anisotropic superconductors, *Physical Review B* **40**, 6695 (1989).

[20] M. A. Tanatar, D. Torsello, K. R. Joshi, S. Ghimire, C. J. Kopas, J. Marshall, J. Y. Mutus, G. Ghigo, M. Zarea, J. A. Sauls, and R. Prozorov, Anisotropic superconductivity of niobium based on its response to non-magnetic disorder (2022), arXiv:2207.14395 [cond-mat, physics:quant-ph].

[21] M. Zarea, H. Ueki, and J. A. Sauls, Effects of anisotropy and disorder on the superconducting properties of niobium, *Frontiers in Physics* **11**, 10.3389/fphy.2023.1269872 (2023).

[22] C. D. Wilen, S. Abdullah, N. A. Kurinsky, C. Stanford, L. Cardani, G. D'Imperio, C. Tomei, L. Faoro, L. B. Ioffe, C. H. Liu, A. Opremcak, B. G. Christensen, J. L. DuBois, and R. McDermott, Correlated charge noise and relaxation errors in superconducting qubits, *Nature* **594**, 369 (2021).

[23] J. Clarke, Experimental Observation of Pair-Quasiparticle Potential Difference in Nonequilibrium Superconductors, *Physical Review Letters* **28**, 1363 (1972).

[24] M. Tinkham and J. Clarke, Theory of Pair-Quasiparticle Potential Difference in Nonequilibrium Superconductors, *Physical Review Letters* **28**, 1366 (1972).

[25] C. C. Chi and J. Clarke, Quasiparticle branch mixing rates in superconducting aluminum, *Physical Review B* **19**, 4495 (1979).

[26] C. C. Chi and J. Clarke, Addendum to "Quasiparticle branch mixing rates in superconducting aluminum", *Physical Review B* **21**, 333 (1980).

[27] T. R. Lemberger and J. Clarke, Charge-imbalance relaxation in the presence of a pair-breaking interaction in superconducting AlEr films, *Physical Review B* **23**, 1088 (1981).

[28] M. Stuivinga, J. E. Mooij, and T. M. Klapwijk, Non-equilibrium potentials of phase-slip centers in superconducting Al strips, *Physica B+C* **108**, 1023 (1981).

[29] J. A. Pals, K. Weiss, P. M. T. M. van Attekum, R. E. Horstman, and J. Wolter, Non-equilibrium superconductivity in homogeneous thin films, *Physics Reports* **89**, 323 (1982).

[30] K. E. Gray, Enhancement of superconductivity by quasiparticle tunneling, *Solid State Communications* **26**, 633 (1978).

[31] J. Fuchs, P. W. Epperlein, M. Welte, and W. Eismenger, Energy Gap Reduction in Superconducting Tin Films by Quasiparticle Injection, *Physical Review Letters* **38**, 919 (1977).

[32] C. J. Pethick and H. Smith, Relaxation and collective motion in superconductors: A two-fluid description, *Annals of Physics* **119**, 133 (1979).

[33] M. Tinkham, *Introduction to Superconductivity*, 2nd ed. (Dover Publications, 2004).

[34] P. Cadden-Zimansky, Z. Jiang, and V. Chandrasekhar, Charge imbalance, crossed Andreev reflection and elastic co-tunnelling in ferromagnet/superconductor/normal-metal structures, *New Journal of Physics* **9**, 116 (2007).

[35] F. Hübner, J. C. Lemyre, D. Beckmann, and H. v. Löhneysen, Charge imbalance in superconductors in the low-temperature limit, *Physical Review B* **81**, 184524 (2010).

[36] M. J. Wolf, F. Hübner, S. Kolenda, H. V. Löhneysen, and D. Beckmann, Spin injection from a normal metal into a mesoscopic superconductor, *Physical Review B* **87**, 024517 (2013).

[37] M. Kuzmanović, B. Y. Wu, M. Weideneder, C. H. L. Quay, and M. Aprili, Evidence for spin-dependent energy transport in a superconductor, *Nature Communications* **11**, 4336 (2020).

[38] J. P. Pekola, D. V. Anghel, T. I. Suppula, J. K. Suoknuuti, A. J. Manninen, and M. Manninen, Trapping of quasiparticles of a nonequilibrium superconductor, *Applied Physics Letters* **76**, 2782 (2000).

[39] K. Lang, S. Nam, J. Aumentado, C. Urbina, and J. Martinis, Banishing quasiparticles from Josephson-junction qubits: Why and how to do it, *IEEE Transactions on Applied Superconductivity* **13**, 989 (2003).

[40] R.-P. Riwar, A. Hosseinkhani, L. D. Burkhardt, Y. Y. Gao, R. J. Schoelkopf, L. I. Glazman, and G. Catelani, Normal-metal quasiparticle traps for superconducting qubits, *Physical Review B* **94**, 104516 (2016).

[41] M. Bal, A. A. Murthy, S. Zhu, F. Crisa, X. You, Z. Huang, T. Roy, J. Lee, D. van Zanten, R. Pilipenko, I. Nekrashevich, A. Lunin, D. Bafia, Y. Krasnikova, C. J. Kopas, E. O. Lachman, D. Miller, J. Y. Mutus, M. J. Reagor, H. Cansizoglu, J. Marshall, D. P. Pappas, K. Vu, K. Yadavalli, J.-S. Oh, L. Zhou, M. J. Kramer, F. Q. Lecocq, D. P. Goronzky, C. G. Torres-Castanedo, G. Pritchard, V. P. Dravid, J. M. Rondinelli, M. J. Bedzyk, M. C. Hersam, J. Zasadzinski, J. Koch, J. A. Sauls, A. Romanenko, and A. Grassellino, Systematic Improvements in Transmon Qubit Coherence Enabled by Niobium Surface Encapsulation (2024), arXiv:2304.13257 [cond-mat, physics:quant-ph].

[42] M. C. de Ory, D. Rodriguez, M. T. Magaz, D. Granados, V. Rollano, and A. Gomez, Low loss hybrid Nb/Au superconducting resonators for quantum circuit applications (2024), arXiv:2401.14764 [cond-mat, physics:quant-ph].

[43] R.-P. Riwar, L. I. Glazman, and G. Catelani, Dissipation by normal-metal traps in transmon qubits, *Physical Review B* **98**, 024502 (2018).

[44] A. Hosseinkhani, R.-P. Riwar, R. J. Schoelkopf, L. I. Glazman, and G. Catelani, Optimal Configurations for Normal-Metal Traps in Transmon Qubits, *Physical Review Applied* **8**, 064028 (2017).

[45] R.-P. Riwar and G. Catelani, Efficient quasiparticle traps with low dissipation through gap engineering, *Physical Review B* **100**, 144514 (2019).

[46] S. Kolenda, M. J. Wolf, D. S. Golubev, A. D. Zaikin, and

D. Beckmann, Nonlocal transport and heating in superconductors under dual-bias conditions, *Physical Review B* **88**, 174509 (2013).

[47] R. C. Dynes, V. Narayanamurti, and J. P. Gorno, Direct Measurement of Quasiparticle-Lifetime Broadening in a Strong-Coupled Superconductor, *Physical Review Letters* **41**, 1509 (1978).

[48] R. Meservey and P. M. Tedrow, Spin-polarized electron tunneling, *Physics Reports* **238**, 173 (1994).

[49] A. A. Golubov and E. P. Houwman, Quasiparticle relaxation rates in a spatially inhomogeneous superconductor, *Physica C: Superconductivity* **205**, 147 (1993).

[50] N. Ashcroft and N. Mermin, *Solid State Physics* (Cengage Learning, 2011).

[51] B. L. Al'tshuler and A. G. Aronov, Magnetoresistance of thin films and of wires in a longitudinal magnetic field, *JETP Letters* **33**, 515 (1981).

[52] B. L. Altshuler, A. G. Aronov, and D. E. Khmelnitsky, Effects of electron-electron collisions with small energy transfers on quantum localisation, *Journal of Physics C: Solid State Physics* **15**, 7367 (1982).

[53] S. Wind, M. J. Rooks, V. Chandrasekhar, and D. E. Prober, One-Dimensional Electron-Electron Scattering with Small Energy Transfers, *Physical Review Letters* **57**, 633 (1986).

END MATTER

Appendix: Scattering Rate Calculations—To calculate the scattering rates obtained in Fig. 6 of the main text, we first determine the electronic mean free path l_{mfp} from the sheet resistance R_{\square} and established values for Al [50], with which we can extract the normal electron diffusion coefficient in the control sample $D_N = v_f l_{mfp}/3$. These quantities are reported in Tab. I.

	R_{\square}	w	d	l_{mfp}	D
Control	6.21 Ω	275 nm	20 nm	3.17 nm	21.5 $\text{cm}^2 \text{s}^{-1}$
Bilayer	7.99 Ω	300 nm	23 nm	[†] 2.47 nm	[†] 16.7 $\text{cm}^2 \text{s}^{-1}$

TABLE I. Measured and Drude model calculated values for both control and bilayer devices. [†]Approximate values for the bilayer calculated using the reported properties of Al alone.

The diffusion coefficient for quasiparticles is energy dependent: $D(\epsilon) = D_N \times \epsilon / \sqrt{\epsilon^2 + \Delta^2}$ [33]. To account for this, we assume that the quasiparticle energy ϵ is $\approx eV_A$ during injection. Taking this, we calculate the charge imbalance time to be $\lambda_{Q^*}^2 / D(eV_A) \equiv \tau_{Q^*}$, to which we apply Eq. 5 using the measured Δ and T_c values reported in Figs. 2 and 3 to estimate the inelastic rate τ_E^{-1} .

Interestingly, the inelastic scattering rates obtained by this calculation, while consistent in magnitude to other reports [35], are inconsistent with the rate of inelastic electron-electron scattering τ_{ee}^{-1} for Al at 20 mK. Considering the predicted inelastic electron-electron scattering rate for a 1D wire [51]

$$\frac{1}{\tau_{ee}} = \frac{1}{\pi^3} \frac{1}{\sqrt{2}} \frac{R_{\square}}{\hbar/e^2} \frac{D}{wL_T}, \quad (\text{A.7})$$

written in terms of the Thouless length $L_T = \sqrt{\hbar D/k_B T}$, we find a rate τ_{ee}^{-1} for our control device of only $3.0 \times 10^5 \text{ s}^{-1}$. Thus, inelastic electron-electron scattering is insufficient to explain the relaxation of quasiparticles in our control device by almost three orders of magnitude.

If we instead consider the Nyquist electron-electron scattering rate [52] (which is not entirely inelastic):

$$\frac{1}{\tau_N} = \left(\frac{1}{\sqrt{2}} \frac{R_{\square}}{\hbar/e^2} \frac{\sqrt{D^3}}{wL_T^2} \right)^{2/3} \quad (\text{A.8})$$

using the same values, we find a rate of $3.4 \times 10^7 \text{ s}^{-1}$. This is within a factor of 2-3 of the measured τ_E^{-1} . This is curious, as the Nyquist rate is more closely related to dephasing of electrons by small energy transfers [53] than to the energy relaxation mechanisms originally assumed by Tinkham [24] and similar works. A detailed study of the full temperature dependence of τ_{Q^*} would be necessary to understand these relationships further.

In light of the theory of Golubov and Houweman [49], predicting that the bilayer rate may be determined primarily by the fastest scattering rate of the two materials, we have attempted to estimate the possible Nyquist rate of the Cu layer in our device. As the R_{\square} value could not be measured independently, we instead prepared 1 cm^2 Cu films of both 3 nm and 10 nm thicknesses under approximately identical growth conditions to those of the bilayer device. Tests of the 3 nm Cu film indicated an immeasurably high sheet resistance, suggesting that the Cu film in our bilayer device may be below the percolation limit. Conversely, the 10 nm Cu film had a sheet resistance of only 2.0 Ω , indicating the deposited film to be of fair quality and fully metallic.

If we were to extrapolate from this, the 3 nm Cu in our bilayer would have $R_{\square} \approx 6.7 \Omega$, which corresponds to a diffusion constant of $170 \text{ cm}^2 \text{s}^{-1}$. This yields a Nyquist rate of $1.3 \times 10^8 \text{ s}^{-1}$, an enhancement over the measured inelastic rate. However, this is likely to be a significant underestimation if the actual 3 nm Cu film is below the percolation threshold, whereupon Coulomb blockade effects should give rise to a large enhancement of inelastic scattering in the bilayer which warrants further study.